



US Army Corps  
of Engineers®

## A Geology-Based Estimate of Connate Water Salinity Distribution

*by Hwai-Ping Cheng, Kevin D. Winters, Stephen M. England,  
Ryan E. Pickett, Mark D. Shafer, and Tricia M. North*

**PURPOSE:** The purpose of this Coastal and Hydraulics Engineering Technical Note (CHETN) is to document a geology-based interpolation method developed to estimate the salinity distribution of connate water with limited number of field data, where the estimated salinity distribution can be used subsequently in groundwater modeling for decision making.

**BACKGROUND:** Connate water is the water entrapped in the interstices of sedimentary rocks at the time of deposition (when the rocks were formed). This water often has a high mineral content and can be exceedingly saline in rock formed under marine conditions. This poses serious environmental concerns if connate water is mobilized into shallow aquifers or surface water systems.

Estimating the distribution of connate water is necessary for evaluating connate water migration due to disturbances, whether or not they are human induced. The estimation method presented in this technical note was developed to provide an estimated distribution of connate water by associating limited salinity data with the layered geologic model developed using much more comprehensive information. The goal of this approach is to use alternative information sources (in this case, the geologic layering) to inform the estimation of the salinity distribution throughout the model domain rather than simply interpolating from a limited set of data points.

The connate water distribution estimated with this method has been used in simulating for density-dependent groundwater flow and salinity transport near the Herbert Hoover Dike (HHD) surrounding Lake Okeechobee in Florida. The simulations were conducted using the subsurface module of the WASH123D model (Yeh et al. 2006). The HHD groundwater modeling was conducted to investigate the impact from the installation of a cutoff wall along the HHD on the groundwater flow patterns near the HHD. In this locality, changes in groundwater flow have the potential for mixing or movement of trapped connate water underlying parts of the area near the HHD, and changes in groundwater flow patterns could potentially degrade the municipal water supply and contaminate groundwater resources used for agricultural production in the Everglades Agricultural Area (EAA).

**Data Constraint.** Because measuring data within the groundwater system is costly and time consuming, estimation of the salinity of connate water using interpolation and extrapolation from a limited number of measurements is unavoidable. Usually, sensitivity analyses are incorporated into model simulations to account for data uncertainty from assumptions in the process of interpolation and extrapolation. The interpolation/extrapolation scheme can be further refined as more data become available, which should result in more accurate estimates of the salinity distribution.

<b>Report Documentation Page</b>			Form Approved OMB No. 0704-0188	
<p>Public reporting burden for the collection of information is estimated to average 1 hour per response, including the time for reviewing instructions, searching existing data sources, gathering and maintaining the data needed, and completing and reviewing the collection of information. Send comments regarding this burden estimate or any other aspect of this collection of information, including suggestions for reducing this burden, to Washington Headquarters Services, Directorate for Information Operations and Reports, 1215 Jefferson Davis Highway, Suite 1204, Arlington VA 22202-4302. Respondents should be aware that notwithstanding any other provision of law, no person shall be subject to a penalty for failing to comply with a collection of information if it does not display a currently valid OMB control number.</p>				
1. REPORT DATE <b>SEP 2014</b>	2. REPORT TYPE		3. DATES COVERED <b>00-00-2014 to 00-00-2014</b>	
4. TITLE AND SUBTITLE <b>A Geology-Based Estimate of Connate Water Salinity Distribution</b>			5a. CONTRACT NUMBER	
			5b. GRANT NUMBER	
			5c. PROGRAM ELEMENT NUMBER	
6. AUTHOR(S)			5d. PROJECT NUMBER	
			5e. TASK NUMBER	
			5f. WORK UNIT NUMBER	
7. PERFORMING ORGANIZATION NAME(S) AND ADDRESS(ES) <b>U.S. Army Engineer Research and Development Center, Vicksburg, MS, 39180-</b>			8. PERFORMING ORGANIZATION REPORT NUMBER	
9. SPONSORING/MONITORING AGENCY NAME(S) AND ADDRESS(ES)			10. SPONSOR/MONITOR'S ACRONYM(S)	
			11. SPONSOR/MONITOR'S REPORT NUMBER(S)	
12. DISTRIBUTION/AVAILABILITY STATEMENT <b>Approved for public release; distribution unlimited</b>				
13. SUPPLEMENTARY NOTES				
14. ABSTRACT				
15. SUBJECT TERMS				
16. SECURITY CLASSIFICATION OF:			17. LIMITATION OF ABSTRACT <b>Same as Report (SAR)</b>	
a. REPORT <b>unclassified</b>	b. ABSTRACT <b>unclassified</b>	c. THIS PAGE <b>unclassified</b>	18. NUMBER OF PAGES <b>16</b>	19a. NAME OF RESPONSIBLE PERSON

**Data Used for Salinity Estimation.** Data collected for connate water modeling at the HHD were used herein to demonstrate the salinity estimation method. The data collection effort was a combination of borehole geophysics, discrete sampling from a short screened interval, and straddle packer sampling from fully penetrating wells. As detailed in the HHD Transport Model report (England et al. 2013), each type of data was useful in the salinity analysis; however, each data set also had its own limitations. Table 1 summarizes the data used in the salinity analysis for the HHD project.

<b>Table 1. Data Used To Estimate Connate Water Distribution</b>				
<b>Well Groups (with Well IDs)</b>	<b>Bulk Conductivity</b>	<b>Fluid Conductivity</b>	<b>TDS Concentration</b>	<b>Chloride Concentration</b>
Downhole Geophysics by USGS (USGS Wacker data) (HHD08-R1A-PW-1, HHD08-R1C-PW-1B, HHD08-R1D-PW-1B, HHD10-R3-PW-1_Redo, HHD10-R3-PW-15, HHD10-R2-PW-15, HHD10-R2-PW-1)	Continuous Available on various dates	Continuous Available only on the date of installation	Not collected	Not collected
Downhole Geophysics and Groundwater Samples by USGS (USGS data) (HHD09-R1A-CB3, HHD10-R1B-MW-2-1, HHD11-R1B-MW-1, HHD08-R1C-MW-8D1, HHD11-R1C-MW-1, HHD08-R1D-MW-5D1, HHD11-R1D-MW-3, HHD10-R3-MW-18F1, HHD10-R2-MW-18F1, HHD10-R2-MW-4F1)	Continuous Available on various dates Measured with USGS field device	Available at two depths (except for HHD10-R2-MW-4F1) Measured in USGS lab	Derived by USGS based on fluid conductivity (TDS = 0.65 * fluid cond.)	Available at two depths (except for HHD10-R2-MW-4F1) Measured in USGS lab
Groundwater Samples from USGS and analyzed by IAG (USGS_IAG data) (HHD09-R1A-CB3, HHD10-R1B-MW-2-1, HHD11-R1B-MW-1, HHD08-R1C-MW-8D1, HHD11-R1C-MW-1, HHD08-R1D-MW-5D1, HHD11-R1D-MW-3, HHD10-R3-MW-18F1, HHD10-R2-MW-18F1, HHD10-R2-MW-4F1)	Not collected	Available at two depths (except for HHD10-R2-MW-4F1) Measured in IAG lab	Available at two depths (except for HHD10-R2-MW-4F1) Measured in IAG lab	Available at two depths (except for HHD10-R2-MW-4F1) Measured in IAG lab
Groundwater Straddle Packer Samples by IAG (IAG data) (HHD08-R1A-MW-11, HHD08-R1C-MW-8D, HHD08-R1D-MW-5D, HHD10-R3-MW-4F, HHD10-R3-MW-18F, HHD10-R2-MW-18F, HHD10-R2-MW-4F)	Not collected	Available at 10–13 depths Measured in IAG lab	Available at 6 depths Measured in IAG lab	Available at 6 depths Measured in IAG lab

The U.S. Geological Survey (USGS) conducted borehole geophysics analyses at 10 USGS project-specific wells (special wells) to facilitate the HHD groundwater modeling. These wells were located along the HHD, and data collection commenced in mid-2011. Each of the USGS wells was constructed to a depth of approximately 130 feet (ft) below the land surface with open screens at the bottom 10 ft of the well. Borehole geophysics was employed to collect bulk electrical

conductivity data on a bi-monthly basis from each well. During the sampling events, water quality samples were taken from the screened interval at the base of the well and from a second sampling port at the approximate depth of the freshwater/saline water interface. These discrete sampling intervals were designed to limit vertical fluid transport within the well borehole. The water quality data collected at each of these special wells included fluid (specific) conductivity and chloride concentration. A USGS laboratory analyzed this data. The groundwater samples collected at these special wells were also sent to the International Analytical Group, Inc. (IAG) for laboratory analysis as a cross check for data quality assurance and quality control (QA/QC).

In addition to the sampling at the USGS wells, IAG also collected and analyzed groundwater samples at various depths using the straddle packer technology. This data was collected at 7 wells near the 10 USGS special wells with collection beginning in April 2012. These wells were constructed to a depth of approximately 150 ft below the land surface and were fully screened. Sampling of these wells was done using a 10 ft-long equipment string composed of top and bottom inflatable packers and an air-driven sampling pump. After lowering the sampling string to a specified depth, the packers were inflated to isolate the sample zone, the sampled well interval was purged, and a sample was collected for field and laboratory analysis. Both total dissolved solids (TDS) and chloride concentrations were collected on a bi-monthly basis at specified depths and locations. Moreover, fluid and bulk electric conductivity data collected previously and provided by Mike A. Wacker of USGS at seven pumping wells, HHD08-R1A-PW-1, HHD08-R1C-PW-1B, HHD08-R1D-PW-1B, HHD10-R3-PW-1\_Red, HHD10-R3-PW-15, HHD10-R2-PW-15, and HHD10-R2-PW-1, around the HHD were used to help in the estimation of salinity distribution.

Table 1 groups all the aforementioned wells based on their associated data. The first well group includes the USGS wells yielding the bulk and fluid conductivity data provided by Wacker. The second well group contains the USGS special wells with all data collection and analysis conducted by USGS. The third well group also includes the USGS special wells, but the collected groundwater samples by USGS were sent to IAG for analysis. The last well group comprises the wells monitored by IAG, where the groundwater samples were both collected and analyzed by IAG. For convenience, the data associated with these four groups are named the USGS\_Wacker data, the USGS data, the USGS\_IAG data, and the IAG data, respectively, in this technical note.

Figure 1 depicts the locations of all these wells, where the USGS wells associated with the USGS\_Wacker data are labeled in red, the 10 USGS special wells are in black, and the IAG wells are in blue. Please note that only one symbol is used in the figure to represent the wells that are close to one another. For examples, HHD10-R2-MW-4F1 (GL-332), HHD10-R2-PW-1, and HHD10-R2-MW-4F in Reach 2 are close to one another and are represented by only one symbol in Figure 1.

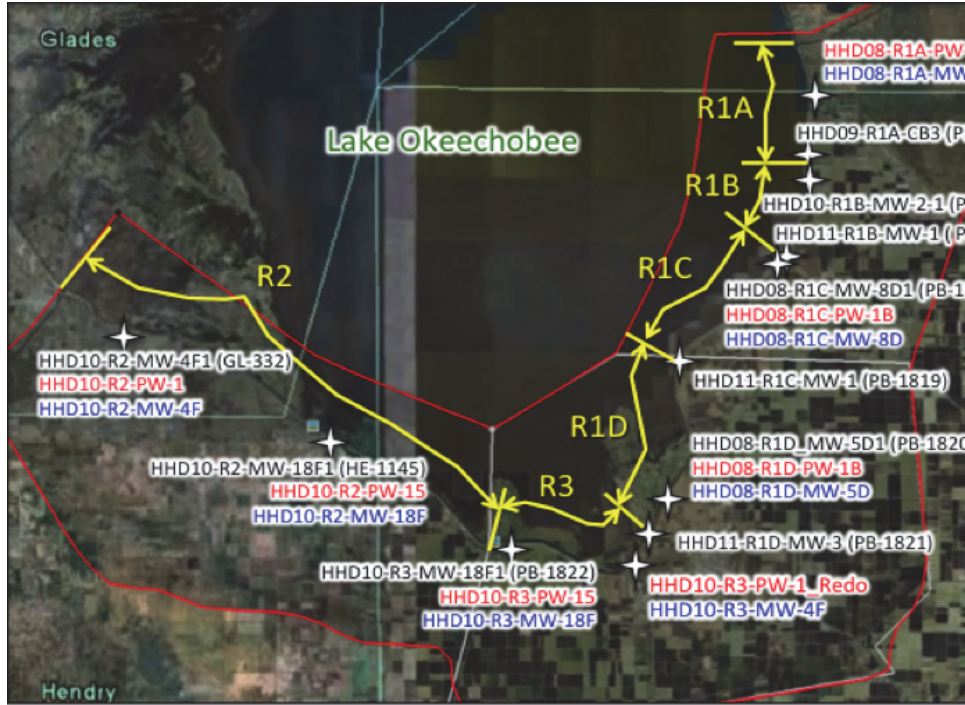


Figure 1. Locations of wells of which observed data are used to estimate connate water distribution in HHD Reaches 1, 2, and 3.

**Data Analysis.** Through data analysis, as detailed in the HHD Transport Model report (England et al. 2013), it was determined that specific conductivity and TDS concentration can be considered to be linearly correlated. By taking into account data from both the USGS and the IAG wells, the following relationship was obtained:

$$[TDS] = 0.684 \times (\text{Specific Conductivity}) \quad (1)$$

where  $[TDS]$  is used to represent TDS concentration; TDS concentration and specific conductivity are in units of milligrams per liter (mg/l) and micro-siemens per centimeter ( $\mu\text{S}/\text{cm}$ ), respectively. As shown in the entry corresponding to the “TDS Concentration” column and the “USGS data” row in Table 1, USGS used 0.65 as the linear coefficient to relate TDS concentration to specific conductivity as a general practice, whereas the authors’ linear coefficient is 0.684 as shown in Equation 1.

By taking  $[TDS] = 35,000 \text{ mg/l}$  as the reference concentration to represent the average seawater salinity, relative salinity  $[RS]$  can be computed as

$$[RS] = \frac{[TDS]}{35000} = \frac{0.684 \times (\text{Specific Conductivity})}{35000} \quad (2)$$

where  $[RS] = 1$  typifies the salinity of seawater.

The comparison of data from the short-screen USGS wells and the fully screened IAG wells demonstrates the mixing within the borehole of a long-screen well (Lapham et al. 1997;

McIlvride and Rector 1988; Oki and Presley 2008; Shalev et al. 2009). As a result, the specific conductivity or concentration data associated with the IAG samples do not accurately represent the salinity of local groundwater. The USGS\_Wacker data was thus employed to generate an estimated distribution of salinity because the associated USGS wells are short-screen wells, and the USGS\_Wacker data has a measurement resolution of 0.1 ft over vertical ranges that covered the HHD modeling domains.

**METHODOLOGY:** Figure 2 depicts the [RS] profile at the USGS well HHD08-R1A-PW-1 as an example from the USGS\_Wacker data, where the [RS] values, expressed in percentages, were calculated using Equations 1 and 2. Figure 2 also depicts a piecewise linear curve developed to approximate the [RS] profile. The number of break points used to construct the piecewise linear curve depends on the variation of the [RS] profile. Different [RS] profiles may need different numbers of break points for their respective piecewise linear curves. Figure 3 depicts the seven piecewise linear curves and their break points associated with the seven [RS] profiles derived from the USGS\_Wacker data, where some break points exist in multiple piecewise linear curves and the others do not. To conduct interpolation without sacrificing accuracy due to dropping break points, the unified set of break points from all piecewise linear curves was employed for each of the seven piecewise linear curves. As a result, a total of 47 break points was used, and the relative salinity concentration value at each break point was computed via interpolation based on the piecewise linear curves shown in Figure 3. Figure 4 shows the piecewise linear curves and the 47 break points for all 7 curves. Please note that the [RS] value of the data point with the lowest elevation in Figure 3 was applied to the break points that have even lower elevations. For instance, the data point with the lowest elevation in Figure 3 is at -155 ft NAVD88 for HHD-08-R1C-PW-1B, and the [RS] value of this data point is 95%. Therefore, [RS] = 95% was applied to the three break points having lower elevations in Figure 4 for HHD-08-R1C-PW-1B.

It is hypothesized that the vertical salinity distribution depends highly on the geologic configuration at equilibrium, and the horizontal salinity distribution is strongly linked to aquifer connectivity because groundwater moves within aquifers that are restricted by confining units (e.g., aquitards) from above and below. This hypothesis is valid when distinct geologic layering exists. To verify this, a groundwater model of layered geology with coupled density-dependent flow and salinity transport was developed. A long-term simulation was conducted with a set of fixed boundary conditions (heads for flow and fluxes for transport) until the variation of the computed salinity distribution was negligible. An examination of the salinity distribution at the end of the simulation indicates that the vertical concentration profile is strongly linked with the geologic layering. With this hypothesis, a geology-based estimation of horizontal salinity variation was developed based on the available data. The following procedures describe the development of a geology-based estimate of initial salinity distribution using the piecewise linear curves.

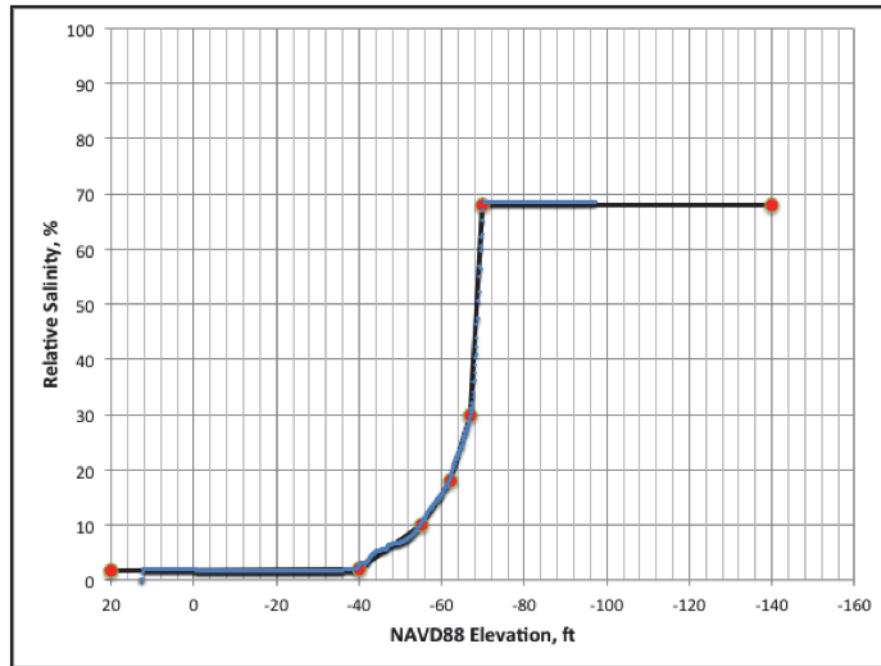


Figure 2. Relative salinity (in %), break points, and the associated piecewise linear curve of HHD08-R1A-PW-1.

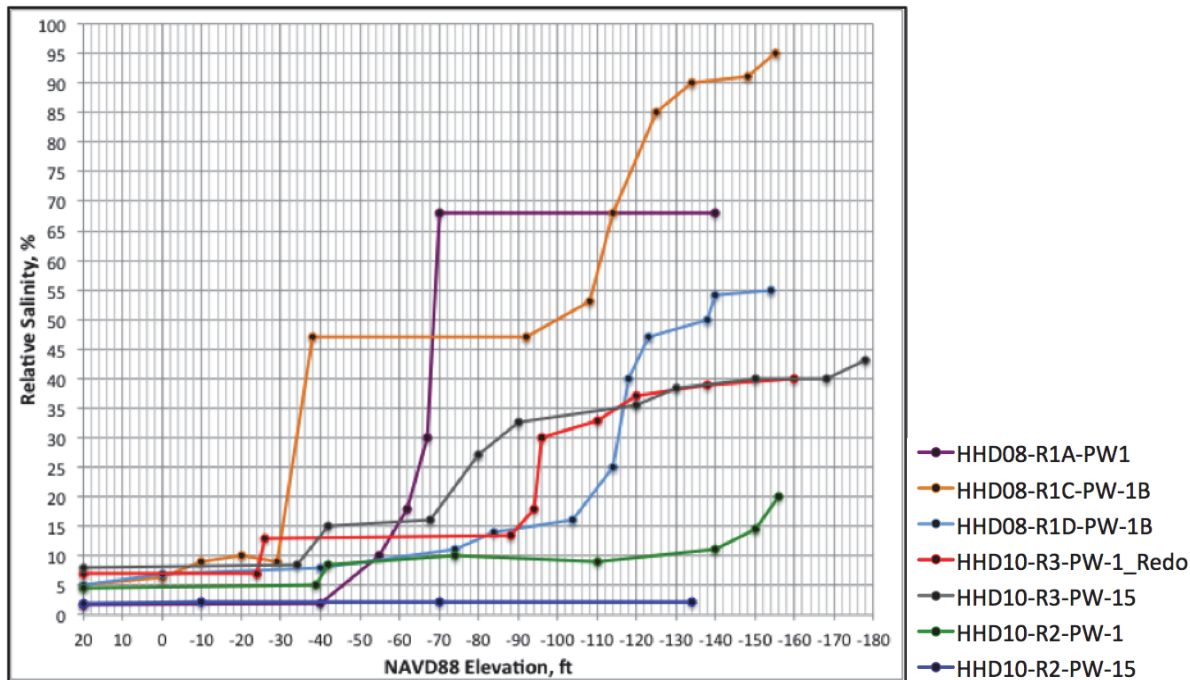


Figure 3. Original break points and the associated piecewise linear curves of the seven wells used to estimate connate water distribution.

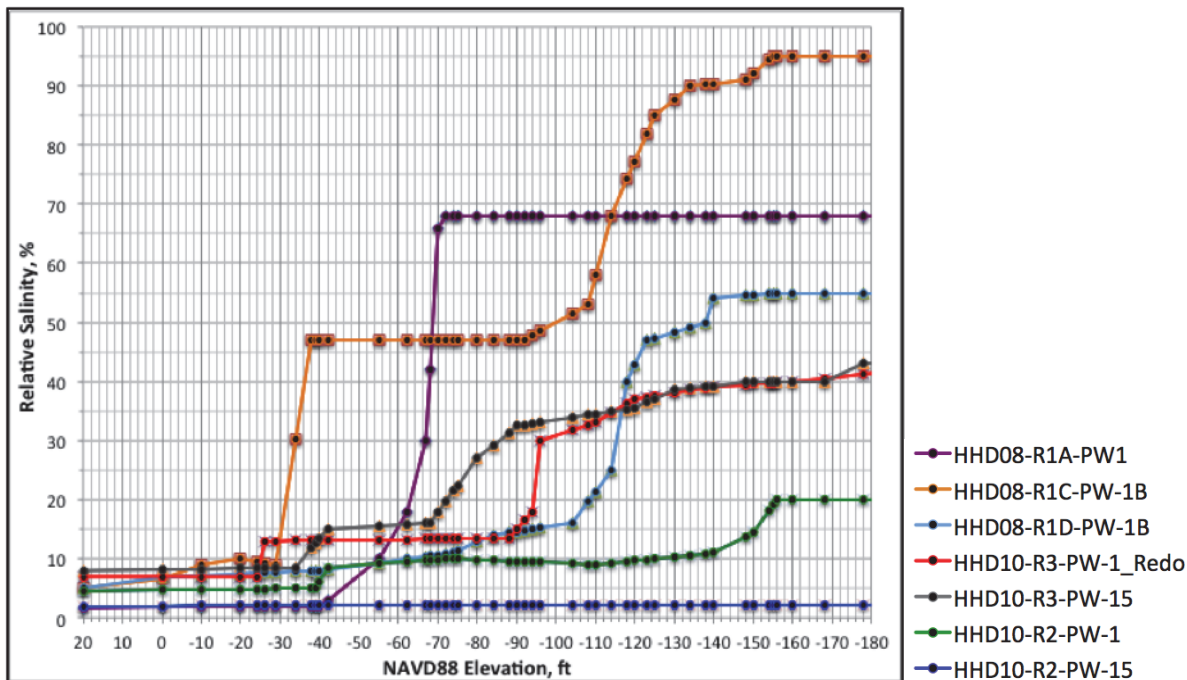


Figure 4. Augmented break points and the associated piecewise linear curves of the seven wells used to estimate connate water distribution. Note that the final sampled value was used as the value for all depths below the sample range (see Figure 3.)

**Procedure 1 - Derivation of Geology-Based Salinity Distribution.** Like most groundwater models, the conceptual geologic model developed for the HHD groundwater modeling has a layered structure (i.e., each geologic layer is represented by a fixed number of element layers vertically, which was incorporated into the finite element computational mesh). For example, the HHD Reach 1B (R1B) model shown in Figure 5 was conceptualized to have 8 geologic units and was discretized with 18 elemental layers:

- 2 for the “Undifferentiated Fill” layer
- 2 for the “Peat/Silt” layer
- 3 for the “Zone 1” layer
- 3 for the “Confining Unit 1” layer
- 2 for the “Zone 2” layer
- 2 for the “Confining Unit 2” layer
- 2 for the “Zone 3” layer
- 2 for the “Sand” layer.

On the other hand, both the Reach 1D&3 (R1D&3) and the Reach 2 (R2) models have 9 geologic units and 20 elemental layers. The “Zone 1”, “Zone 2”, and “Zone 3” layers are higher permeability layers when compared with the confining unit layers. They are composed of limestone, sands, shells, and sandstone.

As shown in Figure 5, the “Interbedded” layer does not exist in the Reach 1B model but is present and discretized with two elemental layers in the R1D&3 and the R2 models. As a result, there are

21 vertical node layers in the R1D&3 and R2 models: the top layer of nodes in the models represents the land surface topography; the 3<sup>rd</sup>, 5<sup>th</sup>, 7<sup>th</sup>, 10<sup>th</sup>, 13<sup>th</sup>, 15<sup>th</sup>, 17<sup>th</sup>, 19<sup>th</sup> are at the interface between two geologic layers; and the 21<sup>st</sup> layer of nodes is at the bottom of the model (located at the interface with the top of the Hawthorne Group). Each node layer can be thought of as a geologic plane. For convenience, a geologic break point is defined as the intersection of a geologic plane and the vertical line at a well point. For R1D&3 and R2 models, therefore, there are 21 geologic break points each at the 7 well points. The [RS] value at a geologic break point can thus be computed via interpolation using the piecewise linear curve of the well point owning the geologic break point. As a result, the [RS] profiles at the seven well points are defined using geologic break points.

Figure 6 shows the geology-based salinity distribution at the 7 well points using 19 and 21 geologic break points, which are for the interpolation of [RS] at R1B mesh nodes and at R1D&3 and R2 mesh nodes, respectively. Ideally, salinity changes significantly across impermeable layers and remains relatively uniform across highly permeable layers. However, there are salinity jumps across the relatively permeable zone 3 layer and relatively uniform concentrations in the relatively impermeable CU2 layer, as shown in Figure 6 (e.g., the orange-color curve associated with HHD-R1C-PW-1B). This is mainly due to how the piecewise linear curves of connate water (Figure 4) and the geologic layering (Figure 5) were developed. The estimated salinity distribution and the geologic layering may not match precisely because the connate water curves and the geologic model were developed using different data sets with different data densities. Please note that the geologic layering conceptualization is sensitive to the borehole data available for the geologist's interpretation. The modeling team may refine the geologic conceptual model to overcome the mismatch as necessary. Also note that the density of geologic break points dictates the shape of the geology-based salinity profile.

**Procedure 2 – Placement of Auxiliary Points Based on Assumptions.** As shown in Figure 1, all the water quality data were taken from wells along the HHD. For various reasons, no applicable data in the EAA (i.e., away from the HHD on the land side) was available for modeling. By assuming the salinity distribution varies horizontally along the HHD and vertically according to the geological layering, auxiliary points are employed to help develop an initial salinity distribution via interpolation. This assumption is again based upon the presence of the continuity of a layered geologic structure. To achieve this, a transect approximately perpendicular to the HHD was drawn for each of the seven USGS wells (Figure 7), where each section line passed through its respective USGS well. Several auxiliary points were then placed along each section line as interpolation points. Geology-based salinity distribution of the well points obtained from Procedure 1 was assigned to the associated auxiliary points. For example, one auxiliary point was placed on the lake side, and three auxiliary points were placed on the land side of the HHD along the section line associated with HHD08-R1A-PW-1, which is the USGS well north of R1B model as shown in Figure 7. The salinity distribution of HHD08-R1A-PW-1 was thus assigned to these four auxiliary points. One additional section line just west of the R2 model domain was drawn to help generate smooth salinity distribution. This additional section line and the four interpolation points along it were associated with the HHD10-R2-PW-1 well point. As a result, there were in total 41 interpolation points, including the 7 well points and 34 auxiliary points (Figure 7).

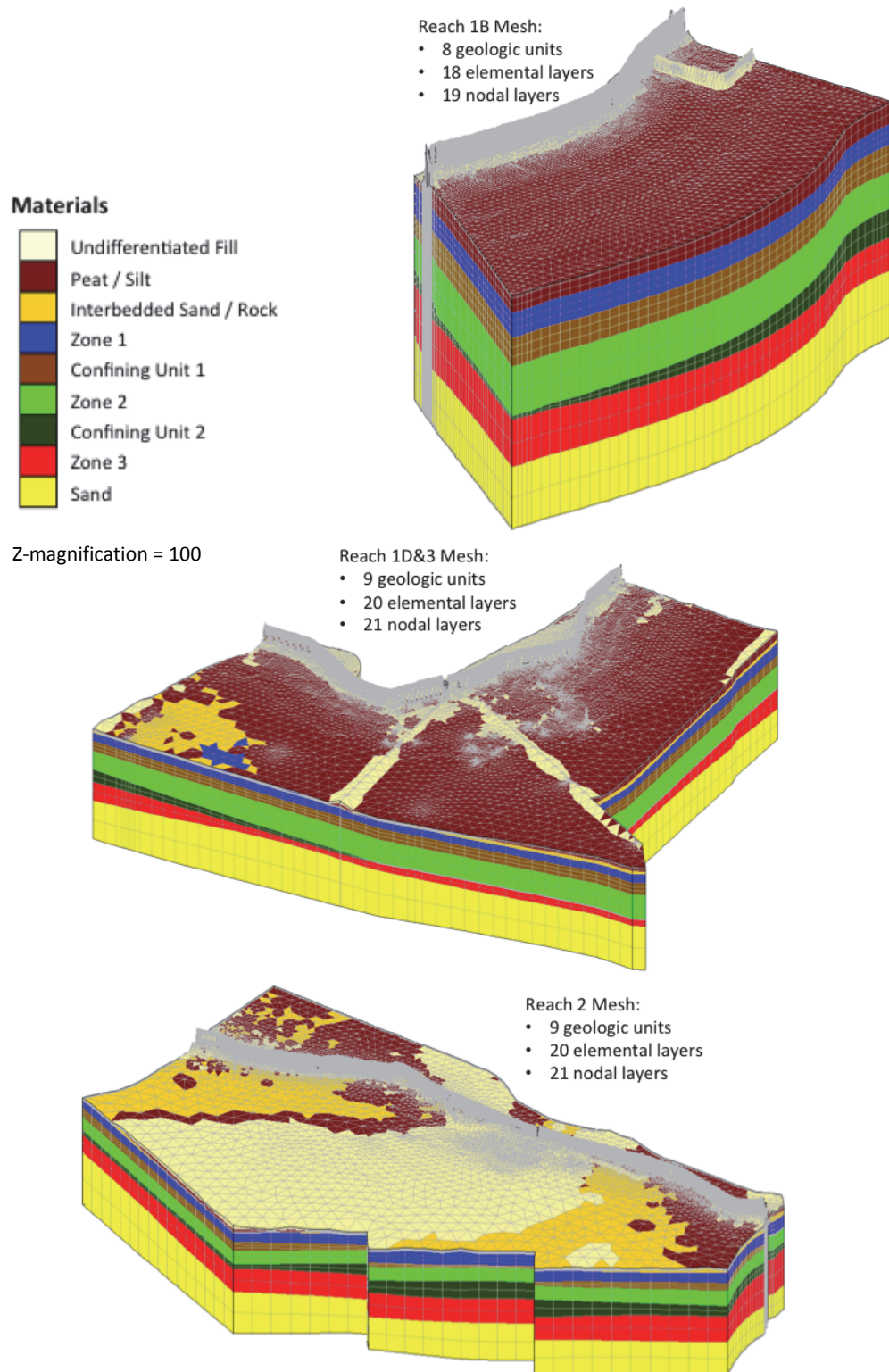


Figure 5. Geologic layering of the HHD Reach 1B, Reach 1D&3, and Reach 2 model computational meshes.

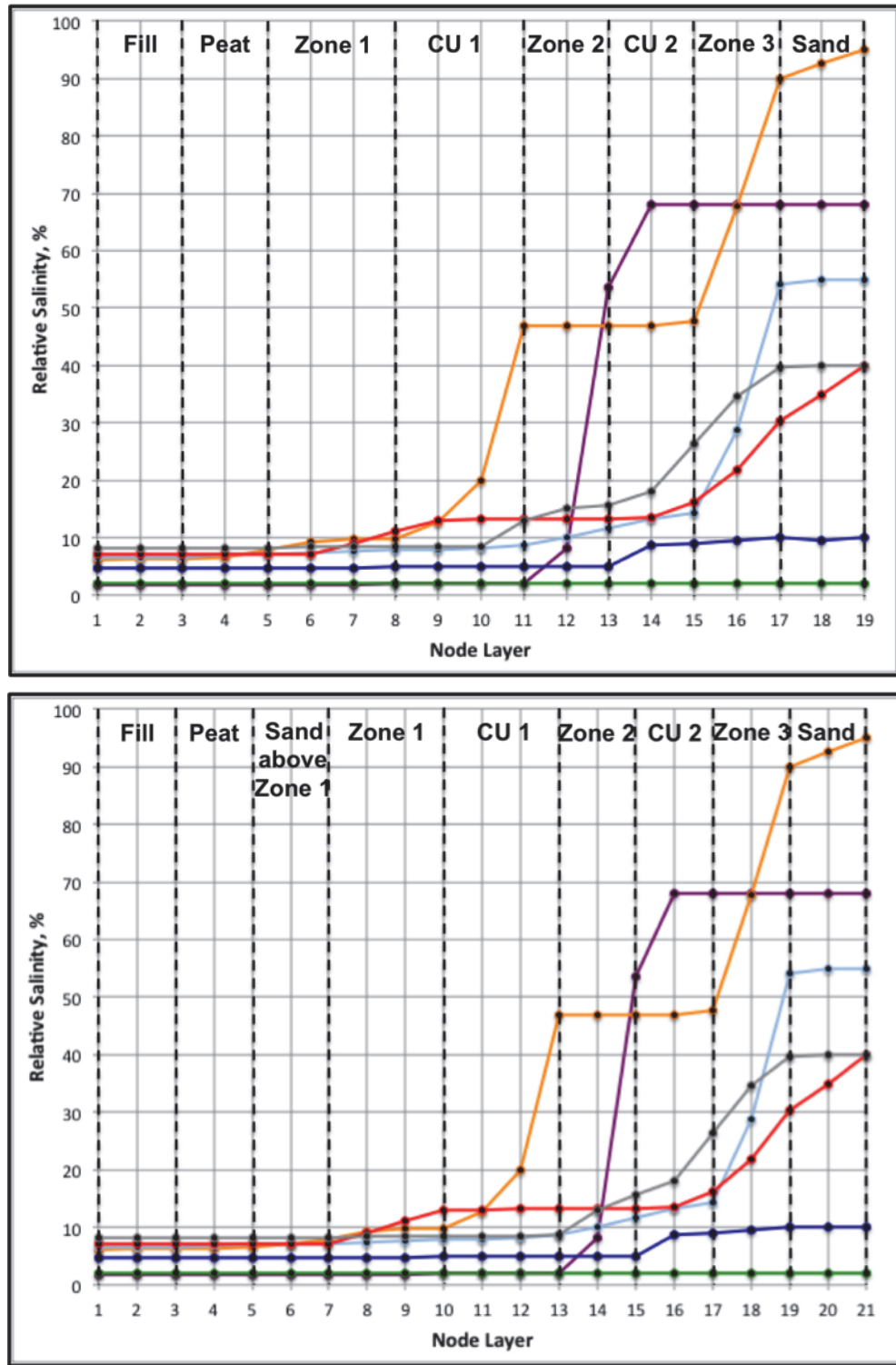


Figure 6. Geology-based interpolation using 19 (top) and 21 (bottom) geologic break points.

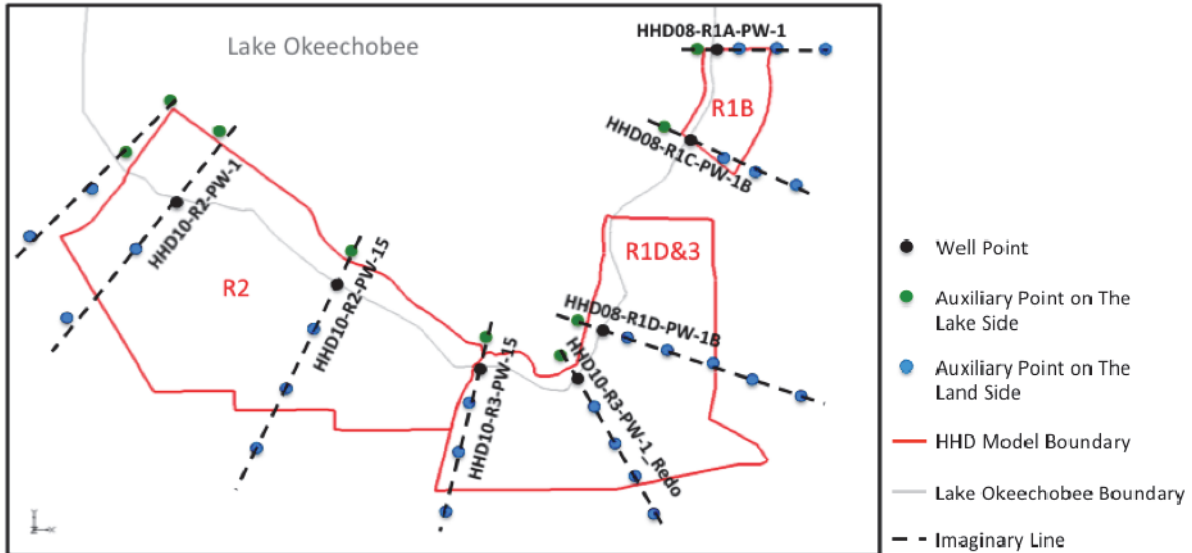


Figure 7. Locations of the 41 interpolation points used for the estimation of connate water distribution.

**Procedure 3 – Interpolation of [RS] at Mesh Nodes.** With a set of interpolation points, the initial salinity at each mesh node can be computed using a user-specified interpolation scheme and the geology-based salinity distribution from Procedure 2. The salinity at a mesh node can be calculated through the following steps.

*Step 1 - Compute the interpolation coefficients based on the X- and Y-coordinates.* Currently the interpolation coefficient associated with an interpolation point given a mesh node with coordinates  $(X_p, Y_p, Z_p)$  is computed as follows:

$$C_i^{X_p, Y_p, Z_p} = \frac{\left[ (X_p - X_i)^2 + (Y_p - Y_i)^2 \right]^{-2}}{\sum_{j=1}^n \left[ (X_p - X_j)^2 + (Y_p - Y_j)^2 \right]^{-2}} \quad (3)$$

where:

$C_i^{X_p, Y_p, Z_p}$  = interpolation coefficient associated with the  $i^{\text{th}}$  interpolation point

$(X_i, Y_i)$  = X- and Y-coordinates of the  $i^{\text{th}}$  interpolation point

$n$  = total number of interpolation points.

This interpolation coefficient is Shepard's Inverse Distance Weighting (IDW, [http://www.emsi.com/gmshelp/Interpolation/Interpolation\\_Schemes/Inverse\\_Distance\\_Weighted/Shepards\\_Method.htm](http://www.emsi.com/gmshelp/Interpolation/Interpolation_Schemes/Inverse_Distance_Weighted/Shepards_Method.htm)) coefficient with a power parameter of 4. To avoid computational error when an interpolation point is closely located to a mesh node, the minimum allowed value for the  $(X_p - X_x)^2 + (Y_p - Y_x)^2$  relationship is  $10^{-6}$  (computed values smaller than this value are replaced by this value).

**Step 2 – Locate the geologic break point associated with the mesh node.** This step identifies the vertical location from a geologic point of view. The mesh node is matched with the geologic break point along the salinity curve. For example, if the mesh node is the 12<sup>th</sup> node from top in the R1B model that has 19 node layers (Figure 6, top plot), it is the middle point of the “Zone 2” layer. If the mesh node is the 12<sup>th</sup> node from top in the R2 model that has 21 node layers (Figure 6, right plot), then it is within the “Confining Unit 1” layer and is on the geologic plane right above the interface of “Confining Unit 1” and “Zone 2” layers. This step assumes that the vertical distribution changes according to the geologic variation as one moves horizontally from the HHD.

**Step 3 – Interpolate [RS] using the interpolation coefficients from Step 1.** After locating the geologic break point in Step 2, the interpolation of [RS] can be performed. This is achieved by using the [RS] values associated with the geologic break points at all interpolation points and the interpolation coefficients computed in Step 1 as follows:

$$[RS]^{X_p, Y_p, Z_p} = \sum_{i=1}^n c_i^{X_p, Y_p, Z_p} [RS]_i^k \quad (4)$$

where  $[RS]^{X_p, Y_p, Z_p}$  is the interpolated RS value at  $(X_p, Y_p, Z_p)$ ,  $[RS]_i^k$  is the [RS] value associated with the  $k^{th}$  geologic break point at the  $i^{th}$  interpolation point.

Figures 8–10 depict the distribution of estimated [RS] on arbitrarily selected cross sections of the R1B, the R1D&3, and the R2 models, respectively, where the three models were generated using the Department of Defense Groundwater Modeling System (GMS). As shown in these figures, the estimated [RS] generally follows the aforementioned assumption: varying horizontally along the HHD and vertically according to the geological layering. Please note that even though the “Peat/Silt”, and the “Interbedded” material zones are exposed at the land surface in certain areas, this interpolation scheme is still applicable. This is because these near-ground-surface materials are present above -20 ft NAVD88, where salinity is low ( $[RS] < 10\%$ , Figure 4).

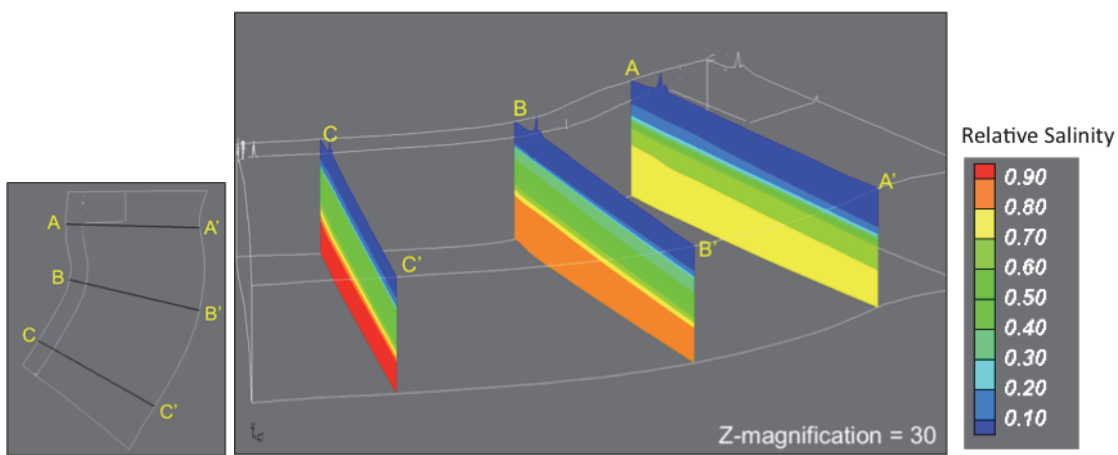


Figure 8. Estimated on three cross sections of the R1B model.

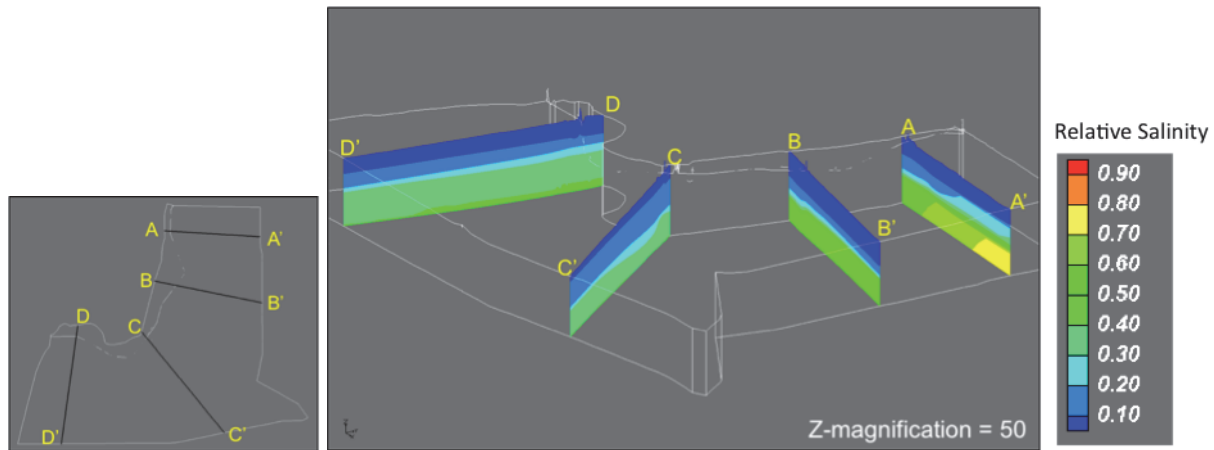


Figure 9. Estimated on three cross sections of the R1D&3 model.

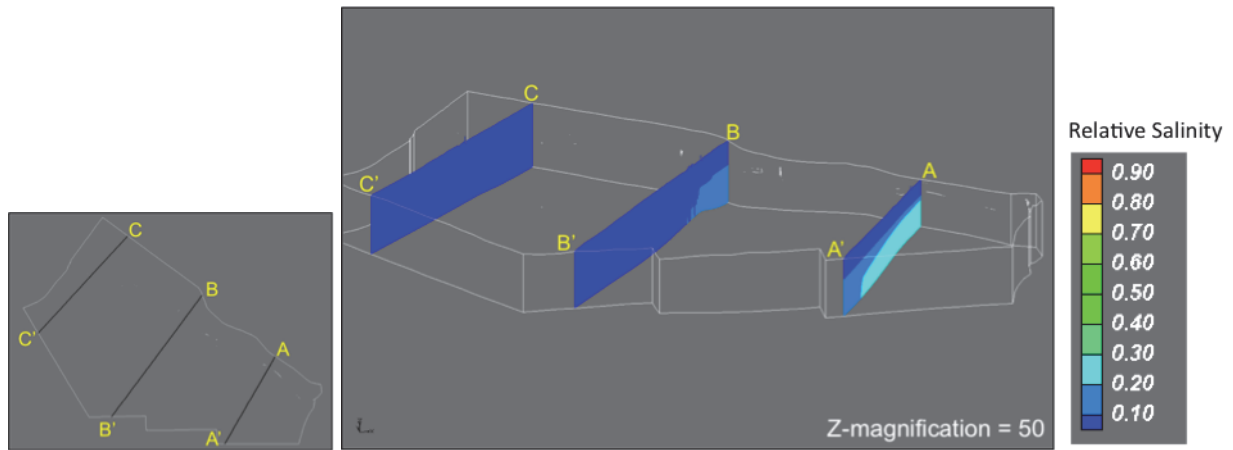


Figure 10. Estimated on three cross sections of the R2 model.

Figure 11 compares the estimated [RS] on six cross sections of the R1D&3 models using the proposed geology-based interpolation (center plot) and the common coordinate-based interpolation (bottom plot). Mostly subtle, yet important, differences between the two estimated [RS] can be seen. A close visual inspection will reveal that the geologic layering approach, used in this paper, has a slightly different distribution of salinity, but the overall effect is to increase the salinity throughout the column, when compared to the coordinate-based approach. Figure 11 also includes the geologic layering of the cross sections (top plot) to verify that the proposed geology-based interpolation generates salinity distribution in accordance with geology.

The estimated [RS] was used as a starting point for the transport modeling in the aforementioned HHD groundwater modeling project. As stated above, this estimated [RS] was developed by assuming a reasonably linear distribution in each geologic layer lakeward and landward of the HHD. This assumption was used because vertical salinity profiles are only available at selected locations near the toe of the HHD. In reality, the flow fields resulting from elevated lake stages and depressed groundwater heads in the EAA will impact this distribution. Using the linearly distributed initial salinity, substantial movement of the salt occurs in the model as the salinity distribution comes into equilibrium with the flow fields. In order to develop a more stable initial

salinity distribution, the estimated [RS] was used as a pre-initial condition to reach a reasonable equilibrium with the current flow fields across the HHD, which is detailed in the HHD Transport Model report (England et al. 2013). It was observed from the authors' numerical experiments that using the estimated [RS] from the geology-based interpolation would reach a reasonable equilibrium quicker than using its counterpart from the coordinate-based interpolation, given the same set of interpolation points.

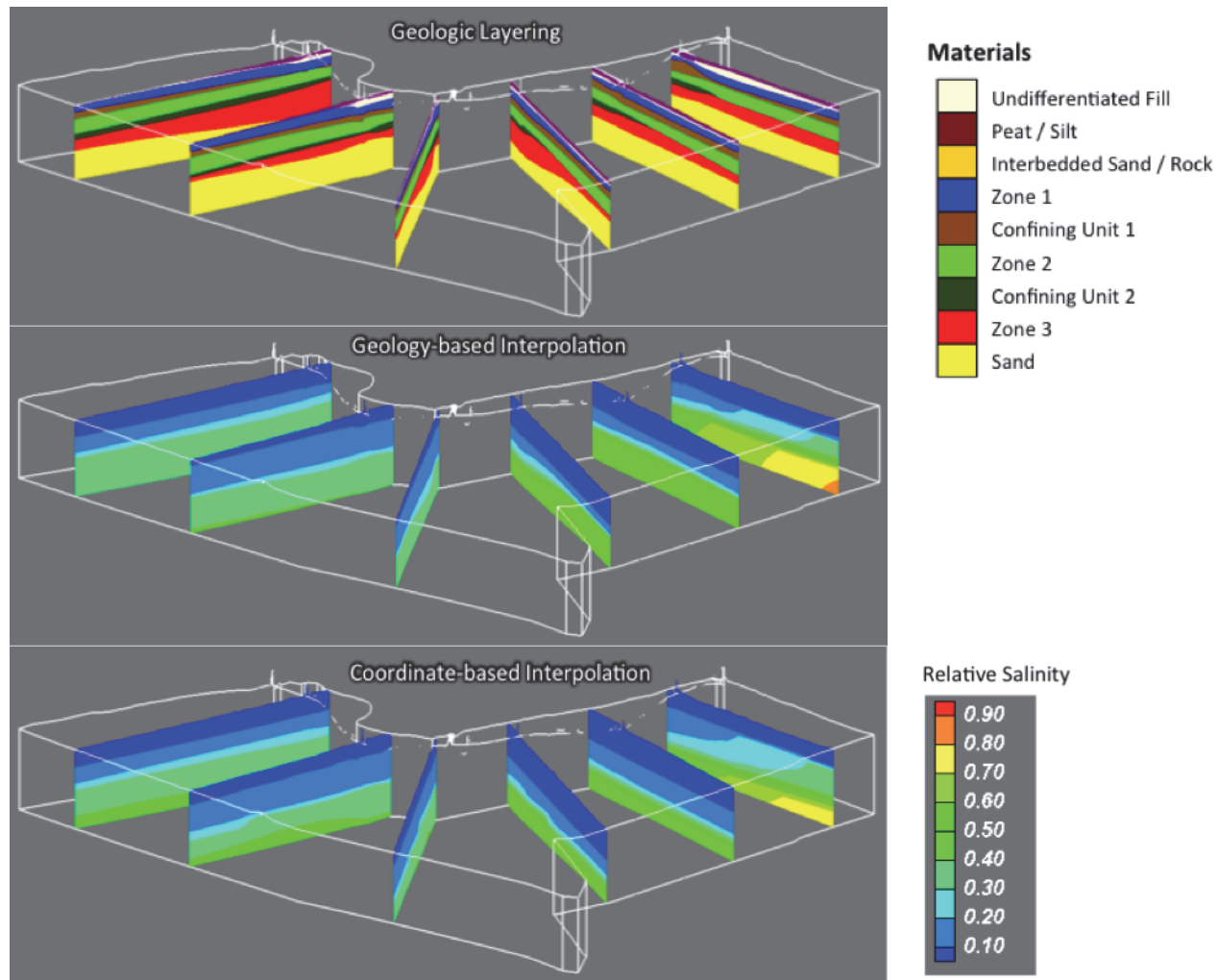


Figure 11. Estimated on six cross sections of the R1D&3 model using geology-based interpolation (center) and coordinate-based interpolation (bottom).

**DISCUSSION:** Frequently in data-sparse situations, there is a need to use alternate sources of data to complement and inform the existing data. This approach uses the significant and physically important geologic layering information to inform the salinity distribution through the subsurface of the HHD. The estimation method stated above is applicable only when strongly layered geologic configurations are present, as is the case for the HHD. It is the modeler's discretion on whether this geology-based estimation is applicable to a model after examining how the vertical distribution of salinity correlates to the geologic layering in the field. The accuracy of the estimation is subject to the number of break points as well as the number of interpolation points used for interpolation. These two numbers are determined by the density of

data, both vertically and horizontally, used to develop the piecewise linear curves. The interpolation result is not unique. Formulations other than Equation 3 can be used to compute interpolation coefficients. Additional field data could improve the resolution of the piecewise linear curves or be used to evaluate the interpolation coefficients.

**SUMMARY:** This technical note presents a geology-based interpolation scheme to facilitate the estimation of the salinity distribution of connate water, in terms of relative concentration (i.e., [RS]), based on limited field data. The estimation method is applicable when layered geologic configurations exist. The method was originally developed for the HHD groundwater modeling project, which required an estimated connate water distribution as the initial condition for the computer simulation of density-dependent flow and salinity transport, so that the impact of a cutoff wall on groundwater flow and connate water migration can be evaluated.

To compute the estimated [RS] value at each of the mesh nodes of the HHD computational model, depth-dependent [RS] profiles were analyzed and converted into piecewise linear curves. Then, a geology-based [RS] distribution was derived from the curves and augmented with auxiliary points. Finally, the [RS] distribution was interpolated to mesh nodes with vertical relevance based on geologic position.

The geology-based interpolation can also be used to provide a quick estimate of the distribution of other quantities (e.g., total head, with limited scattered data available).

**ADDITIONAL INFORMATION:** This work was funded through a Herbert Hoover Dike groundwater modeling project by the U.S. Army Corps of Engineers (USACE), Jacksonville District. Dr. Mark D. Wahl, of the USACE Engineer Research and Development Center (ERDC), Coastal and Hydraulics Laboratory (CHL), and Laura D. Bittner, P.E., Chief of Hydrology, Hydraulics, and Coastal Branch, of the USACE Philadelphia District, reviewed this technical note and provided valuable comments. For additional information, contact Hwai-Ping (Pearce) Cheng, (ERDC), (CHL), 3909 Halls Ferry Road, Vicksburg, MS 39180, at 601-634-3699 or e-mail: [Hwai-Ping.Cheng@usace.army.mil](mailto:Hwai-Ping.Cheng@usace.army.mil).

This CHETN should be cited as follows:

Cheng, H.-P., S. M. England, M. D. Shafer, R. E. Pickett, K. D. Winters, and T. M. North. 2014. *A geology-based estimate of connate water salinity distribution*. ERDC/CHL CHETN-XI-3. Vicksburg, MS: U.S. Army Engineer Research and Development Center.

An electronic copy of this CHETN is available from <http://chl.erdc.usace.army.mil/chetn>.

## REFERENCES

England, S. M., T. M. North, and H.-P. Cheng. 2013. *Herbert Hoover Dike (HHD) transport model*. Project Report submitted to SAJ. Vicksburg, MS: U.S. Army Engineer Research and Development Center.

Lapham, W. W., F. D. Wilde, and M. T. Koterba. 1997. *Guidelines and standard procedures for studies of ground-water quality: Selection and installation of wells, and supporting documentation*. WRI 96-4233. Reston, VA: U.S. Geological Survey.

McIlvride, W. A., and B. M. Rector. 1988. Comparison of short- and long-screen monitoring wells in alluvial sediments. In *Proceedings of the Second National Outdoor Action Conference on Aquifer Restoration, Ground Water Monitoring and Geophysical Methods, 23–26 May, Las Vegas, Nevada*, 1:375–390. Dublin, OH: National Water Well Association.

Oki, D. S., and T. K. Presley. 2008. Causes of borehole flow and effects on vertical salinity profiles in coastal aquifers. In *Program and Proceedings Book of the 20th Salt Water Intrusion Meeting (SWIM), 23–27 June, Naples, Florida*, 170–173. <http://conference.ifas.ufl.edu/swim/papers.pdf>.

Shalev, E., A. Lazar, S. Wollam, S. Kington, Y. Yechieli, and H. Gvirtzman. 2009. Biased monitoring of fresh water-salt water mixing zone in coastal aquifers. *Ground Water* 47(1):49–56.

Yeh, G.-T., G. Huang, H.-P. Cheng, F. Zhang, H.-C. Lin, E. Edris, and D. Richards. 2006. A first-principle, physics-based watershed model: WASH123D. In *Watershed models*, ed. V. P. Singh and D. K. Frevert, 211–244. Boca Raton, FL: CRC Press, Taylor and Francis Group.

**NOTE:** The contents of this technical note are not to be used for advertising, publication, or promotional purposes. Citation of trade names does not constitute an official endorsement or approval of the use of such products.